Membrane Tension Modifies Redox Loading and Release in Single Liposome Electroanalysis

Samuel T. Barlow, Benjamin Figueroa, Dan Fu, and Bo Zhang*

Department of Chemistry, University of Washington, Seattle WA 98195-1700 United States

Liposomes, vesicles, soft nanoparticles, electroporation, osmotic pressure, membrane tension, electrochemistry

ABSTRACT: Here we present a study of how liposomes are loaded and release their contents during their electrochemical detection. We loaded 200 nm liposomes with a redox mediator, ferrocyanide and used amperometry to detect their collision on a carbon-fiber microelectrode (CFE). We found we could control the favorability of their electroporation process and the amount of ferrocyanide released by modifying the osmolarity of the buffer in which liposomes were suspended. Interestingly, we observed that the quantity of released ferrocyanide varied significantly with buffer osmolarity in a non-monotonic fashion. Using stimulated Raman scattering (SRS), we confirmed this behavior was partly explained by fluctuations in intravesicular redox concentration in response to osmotic pressure. To our surprise, the redox concentration obtained from SRS was much greater than that obtained from amperometry, implying that liposomes may release only a fraction of their contents during electroporation. Consistent with this hypothesis, we observed barrages of electrochemical signals that far exceeded the frequency predicted by Poisson statistics, suggesting single liposomes can collide with the CFE and electroporate multiple times. With this study, we have resolved some outstanding questions surrounding electrochemical detection of liposomes while extending observations from giant unilamellar vesicles (GUVs) to 200 nm liposomes with high temporal resolution and sensitivity.

INTRODUCTION

Liposomes are soft nanoparticles comprised of a lipid bilayer (~5 nm thick) enclosing an aqueous solution compartment. Liposomes are specifically useful as mimics for cell membranes, enabling the controlled study of diverse phenomena in membrane biophysics.[1] For example, giant unilamellar vesicles (GUVs, 1-200 μm diameter) can be readily observed with optical microscopy, making them useful for understanding dynamic membrane behavior such as phase separation,[2,3] domain formation,[4-6] and electroporation.[7-9] Conversely, small unilamellar vesicles (SUVs, 20-100 nm diameter) have been used as analogs for synaptic vesicles (30-50 nm diameter) to understand membrane fusion.[10-13]

Electrochemistry has recently emerged as a powerful technique for studying redox-containing liposomes (100-400 nm diameter). Electrochemical methods, such as amperometry, have high temporal resolution (sub-millisecond) and low limits of detection (down to a few thousand molecules).[14] Thus, amperometry has been useful for the direct quantitation of redox-active liposome contents as well as understanding how liposomes open during collision with an ultramicroelectrode (UME) surface.[15-17]

However, key questions remain in collision-based electrochemical detection of liposomes. What is the detection mechanism for liposomes colliding with an UME? It is critical to note that electrochemical detection of liposome contents requires the opening of the lipid bilayer upon collision – otherwise, contents will not be electrolyzed, as the lipid bilayer is too thick for efficient electron tunneling unless other electroactive dopants or defects are introduced.[18-21] Consistent with this, Lebegué et al. showed that they failed to detect 100 nm DMPC liposomes upon collision with a Pt UME unless a sufficient concentration of surfactant was present, implying that membrane destabilization is critical to detection.[22] More recent work extended these results and added temperature and additional redox probes in solution as possible methods for membrane permeabilization.[23] By contrast, Cheng and Compton used carbon-fiber microelectrodes (CFEs) to detect commercial liposomes containing ascorbate; they demonstrated quantitative detection without any destabilizing agents present and suggested a

detection mechanism due to complete membrane rupture of the liposome upon collision.[24] The Ewing group used CFEs to detect liposomes loaded with dopamine (DA) but suggested an electroporation-based mechanism due to the dependence of detection frequency on applied potential.[25]

Critically, it is also unclear how liposomes are loaded with redox molecules and whether liposome detection is quantitative. The Ewing group attempted to load 400 nm liposomes with 150 mM DA, but only detected 40-70% of the expected amount – they attributed the disparity to poor encapsulation efficiency.[25] Our group and the Mirkin group recently published similar results using $K_4Fe(CN)_6$-loaded liposomes; the calculated concentration of $K_4Fe(CN)_6$ based on electrochemical signals was dramatically lower than the expected concentration.[26,27]

We were keenly interested in addressing these key points of liposome loading and release. By using amperometry, we measured the collision of $K_4Fe(CN)_6$-loaded, 200 nm liposomes with a 5 µm CFE. Importantly, the electroporation mechanism suggested by the Ewing group[25] should depend strongly on initial membrane tension, which can be tuned by modifying the osmolarity of the buffer in which liposomes are suspended. *Indeed, we found that we could manipulate the frequency of amperometric events by altering the osmolarity of the buffer, consistent with an electroporation mechanism for liposome detection.* The rate and quantity of $Fe(CN)_6^{4-}$ released during liposome collision/electroporation was also controlled by buffer osmolarity. Significantly, we found that [$Fe(CN)_6^{4-}$] in liposomes varies dramatically with buffer osmolarity, consistent with a recent report.[28] We also provide evidence that single liposomes may release a fraction of their contents, i.e., may be detected more than once, as suggested by the Mirkin group.[27] We believe this work helps clarify detection and loading of redox-filled liposomes, and may be useful for a more complete understanding of electrochemical detection of biological vesicles[29-33] and/or the development of rapid, quantitative techniques for liposome analysis.

MATERIALS AND METHODS

Reagents and Materials. 1,2-Dioleoyl-sn-glycero-3-phosphocholine (DOPC, >99%), 1,2-dioleoyl-sn-glycero-3- phosphethanolamine (DOPE, >99%) and cholesterol (ovine wool) were purchased from Avanti Polar Lipids (USA). Potassium chloride (KCl), HEPES (4-(2-hydroxyethyl)-1-piperazineethanesulfonic acid), ferrocenemethanol (FcMeOH), and potassium hexacyanoferrate(II) trihydrate ($K_4Fe(CN)_6$, ferrocyanide) were purchased from Sigma. All aqueous solutions were prepared using 18.2 MΩ cm^{-1} water and adjusted to pH 7.4 using 1 M KOH. All reagents used were reagent grade or better.

Solutions. Experiments were performed in recording buffer (RB) with base recipe: 0.5 M KCl, 10 mM HEPES, pH 7.4. To change the osmolarity of the recording buffer, we made solutions with 0.1-0.7 M KCl, 10 mM HEPES, pH 7.4, corresponding to osmolarities of 0.2-1.4 osmol (Osm) L^{-1}. *Note*: We assumed 1 Osm L^{-1} (0.5 M KCl, 10 mM HEPES, pH 7.4) to be isotonic relative to the liposome lumen, which is indicated by the dashed vertical line on several figures.

Liposome Synthesis. Lipids dissolved in chloroform were mixed in a mass ratio of 2:1:1 to obtain a concentration of 9.07 mM DOPC, 4.80 mM DOPE, and 9.24 mM cholesterol before chloroform evaporation as described previously. A thin lipid film was formed by evaporating chloroform under N_2 for 30 minutes followed by 2 hours under vacuum dessicator to evaporate any trace organic solvent present in the lipid film. To load liposomes with a redox mediator, the lipid film was hydrated for 1 hour with 2 mL of 500 mM $K_4Fe(CN)_6$, 10 mM HEPES, pH 7.4 and vortexed periodically to support mixing. Hydrated lipid solution was extruded through a 200 nm polycarbonate membrane (Whatman) in a mini-extruder (Avanti) 21 times to obtain 200 nm liposomes. The extruded solution was then diluted to a final volume of 30 mL and centrifuged at 16,000 g for 2 hours to obtain a liposome pellet. Pellet was resuspended in 2 mL of 0.5 M KCl, 10 mM HEPES, pH 7.4. Liposomes could be stored at 4 °C for up to 2 days.

Microelectrode Preparation. CFEs were prepared as described previously[34] by aspirating a carbon fiber (5 µm) into a borosilicate glass capillary (1.2 mm o.d., 0.9 mm i.d., Sutter) that was pulled to a fine tip using a P97 pipet puller (Sutter). Microelectrodes were cut and sealed in epoxy (Epoxy Technologies), followed by 2 h at 80 °C and 2 h at 150 °C to cure. CFEs were polished on a home-built micropipette beveler. CFEs were backfilled with 3 M KCl to establish electrical contact. Electrodes were tested with cyclic voltammetry in 1 mM FcMeOH, 100 mM KCl at 100 mV/s vs. Ag/AgCl. Only electrodes with stable *i-E* curves and good electron-transfer kinetics were used for experiments.

Liposome Collision and Detection. In a typical experiment, the stock suspension of liposomes (suspended in 0.5 M KCl, 10 mM HEPES, pH 7.4) were spiked into a recording buffer of the same or different osmolarity (typically 50× dilution factor). The CFE was immersed in this suspension and poised at E_{app} = +1 V vs. Ag/AgCl unless otherwise indicated.

Data Acquisition and Analysis. Electrodes were held at E_{app} vs. Ag/AgCl using a commercial patch-clamp current amplifier (Axopatch 200B; Axon Instruments). The current was filtered at 2 kHz using an internal low-pass Bessel filter and sampled at 100 kHz using a Digidata 1440 digitizer (Axon Instruments). Amperometric spike characteristics characteristics, including I_{max} (peak amplitude, pA), $t_{1/2}$ (full width of peak at half-maximum, ms), t_{rise} (10–90% max peak height, ms), t_{fall} (90–10% max peak height, ms), and Q (integrated charge, fC) were identified using pClamp v10.6 software (Axon Instruments). Spikes were identified if the I_{max} exceeded 5 times the standard deviation (SD) of the noise. All identified spikes were inspected, and unfit spikes were manually discarded (such as those associated with electrical noise or vibrations). Statistical significance between groups was assessed using the Mann–Whitney–Wilcoxon rank-sum U test (Mann–Whitney) and statistical significance across multiple groups was measured by one-way ANOVA (ANOVA). Statistics are reported as the mean ± SEM (standard error of the mean).

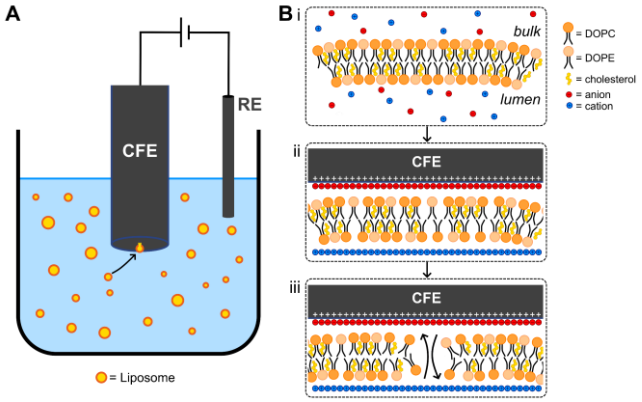

Figure 1. Electrochemical detection of redox-filled liposomes. *A)* Cartoon depicting liposome detection *via* amperometry. A redox-filled liposome diffuses to the CFE surface, where it is electroporated and leaks its contents to the electrode for detection. *B)* Mechanism for electrochemical detection of liposomes *via* electroporation. *i)* Initially, the lipid bilayer separating the liposome contents (lumen) from the external solution (bulk) is in a state of equilibrium. *ii)* The liposome encounters the electrode surface (positively biased). Charging of the bilayer membrane occurs, increasing membrane tension. *iii)* Membrane tension reaches a critical point and the membrane ruptures (electroporation), permitting solution exchange and electrochemical detection of liposome contents.

RESULTS AND DISCUSSION

Redox-Filled Liposomes are Detected Electrochemically via Electroporation. Similar to what has been demonstrated in other works,[22-25,27] we were able to detect freely diffusing, $K_4Fe(CN)_6$-filled liposomes (~200 nm diameter, **Figure S1**) upon collision at a CFE *via* amperometry (**Figure 1A**). The frequency of amperometric signals depended on the applied voltage to the CFE (E_{app}), with no signals observed when E_{app} < +0.4 V vs. Ag/AgCl; the maximum frequency of signals was observed at E_{app} = +1 V, consistent with the cyclic voltammogram (CV) for 5 mM $Fe(CN)_6^{4-}$ (**Figure S2**). Liposomes loaded with buffer free of redox molecules could not be detected (**Figure S3**). The frequency of signals also depended strongly on the concentration of liposomes in solution; when liposomes were diluted 1000× in buffer (see *Methods*), we observed signals at a frequency of 0.04 ± 0.01 s^{-1}; at 50×, the signal frequency was 0.73 ± 0.20 s^{-1} (**Figure S4**, **Table S1**). Taken together, these observations strongly suggest that the observed amperometric signals are the result of single liposome collisions with the CFE surface and subsequent electrolysis of their contents.

To detect redox-filled liposomes on an electrode, the lipid bilayer separating the internal redox contents from the external solution must open. As suggested previously, the most likely mechanism for liposome or vesicle electrochemical detection is *electroporation*, which we describe as follows (**Figure 1B**): *i)* Initially, the internal compartment of liposomes are in a state of equilibrium with the external solution – any differences in the concentration of osmolytes between the liposome lumen and the bulk solution are small enough that the membrane is stable; *ii)* when the liposome encounters the large electric field nanometers from the electrode surface (~10^6 V/cm),[25,35] the lipid membrane behaves as a capacitor, as charged species cannot pass through the bilayer; charges accumulate on either side, increasing the transmembrane voltage and subsequently, membrane tension; *iii)* eventually, the tension energy exceeds the limit of the membrane, causing membrane rupture (electroporation) and leakage of internal contents to the electrode surface, where they are detected.[7-9]

Manipulation of Membrane Tension Modifies Liposome Electroporation. It was shown previously that the critical voltage required for electroporation of liposomes depends strongly on the initial membrane tension.[9] Thus, changing the liposome membrane tension should change the favorability of electroporation and subsequently, the frequency of amperometric events. As our stock of liposomes was

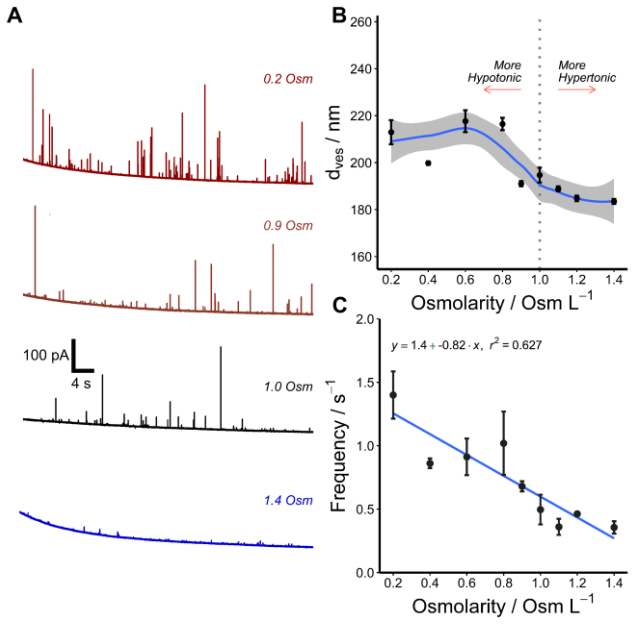

Figure 2. Membrane tension modifies liposome detection. *A)* Example amperometric traces for liposomes suspended in four different osmolarity buffers (E_{app} = +1 V vs. Ag/AgCl). *B)* Using DLS, we determined the average diameter (d_{ves}) of liposomes suspended in different osmolarity buffers. The blue curve is a local regression line (grey shading is SEM) to guide the eye. p = 2.4 × 10^{-7}, ANOVA. *C)* Amperometric detection frequency depended strongly on the osmolarity of the buffer. A linear fit is used to guide the eye. Liposomes were spiked into different osmolarity buffers at a 50× dilution factor. p = 3.22 × 10^{-4}, ANOVA.

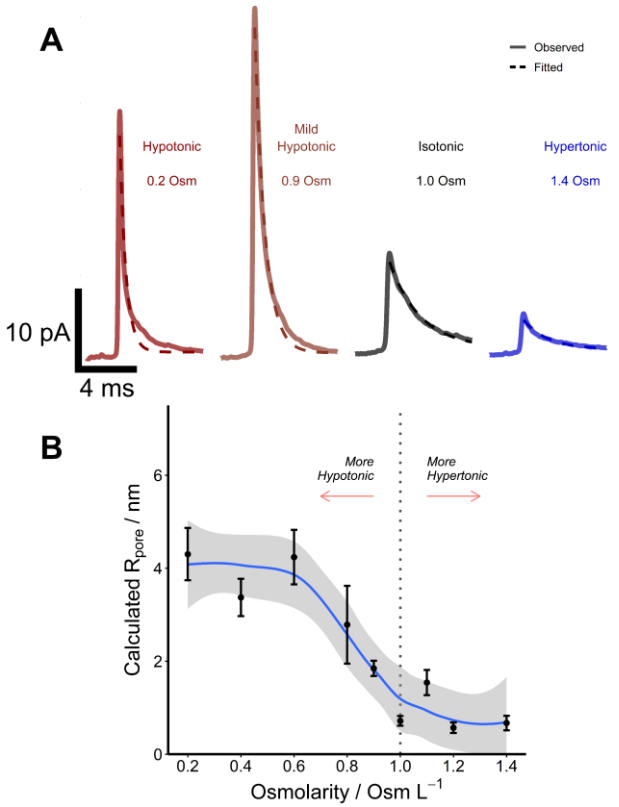

Figure 3. Membrane tension controls peak shape, size of the fusion pore. *A)* Average peaks from liposome detections in four different osmolarity buffers (here, Osm is Osm L^{-1}). A single exponential decay fit is overlaid with a dashed line. *B)* From the time constant, τ, of the exponential decay fit, we can calculate the radius of the fusion pore during electroporation, R_{pore} (see text). R_{pore} is the average of three measurements at each osmolarity. The blue curve is a local regression line (grey shading is SEM) to guide the eye. p = 2.35 × 10^{-5}, ANOVA.

stored in 0.5 M KCl (1 Osm L^{-1}), we reasoned that liposome membrane tension would change when we exposed liposomes to more hypotonic (0.2-0.9 Osm L^{-1}) or hypertonic (1.1-1.4 Osm L^{-1}) buffers relative to the storage buffer (see *Methods*). Measuring liposome size with DLS confirmed this expectation, with the average diameter of liposomes decreasing from 213 ± 5 nm in 0.2 Osm L^{-1}, to 183 ± 1 nm in 1.4 Osm L^{-1} (p = 2.4 × 10^{-7}, ANOVA), consistent with swelling or shrinking behavior associated with hypotonic or hypertonic conditions, respectively.[36]

When we amperometrically detected liposomes suspended at the same concentration (50×) in different osmolarity buffers, we observed a stark decrease in the frequency of detection events, from 1.40 ± 0.19 s^{-1} in 0.2 Osm L^{-1} to 0.36 ± 0.05 s^{-1} in 1.4 Osm L^{-1} (p = 3.22 × 10^{-4}, ANOVA). The variation of event frequency with osmolarity (*despite* similar particle concentrations) suggested electrochemical detection is more favorable when the liposome membrane is more tense, consistent with electroporation (**Figure 2A, C**). For examples of single signals, see **Figure S5**.

Figure 3A shows the average amperometric signal from the oxidation of released $Fe(CN)_6^{4-}$ during liposome collision/electroporation for four selected osmolarities (average peaks at all osmolarities, **Figure S6**). Signal shapes shifted from high amplitude with shorter duration at more hypotonic osmolarities (0.2-0.9 Osm L^{-1}) to low amplitude with longer duration at more hypertonic osmolarities (1.0-1.4 Osm L^{-1}), implying that the fluid junction (fusion pore) that forms during electroporation is wider under hypotonic conditions, facilitating faster flux of molecules out of the liposome (detailed peak statistics, **Figure S7** and **Table S2**).

To quantitatively understand how electroporation behavior changes as a function of

osmolarity, we applied procedures outlined by Amatore and Ewing, to calculate the radius of the fusion pore.[25,37] By fitting the falling phase of the average peaks with an exponential decay function (dashed lines, **Figure 3A**), we extracted the time constant of decay, τ. The maximum pore radius, R_{pore}, is given by the following relationship:

$$R_{pore} = \frac{{R_{lip}}^3}{D_{lip} \times \tau}$$

where R_{lip} is the radius of the liposome at each osmolarity (extracted from DLS sizing, **Figure 2B**); D_{lip} is the diffusion coefficient of $Fe(CN)_6^{4-}$ within the liposome, which we assumed was identical to its coefficient in bulk (D_{lip} = 7.2 × 10^{-6} cm^2 s^{-1}).[38] By our calculation, R_{pore} increased as osmolarity decreased, from 0.7 ± 0.2 nm at 1.4 Osm L^{-1} to 4.3 ± 0.6 nm at 0.2 Osm L^{-1} ($p = 2.35 \times 10^{-5}$, ANOVA).

R_{pore} depended strongly on the initial membrane tension, and interestingly, the ratio of R_{pore} to R_{ves} did not remain constant (e.g. 4.0 ± 0.5 % at 0.2 Osm L^{-1}, 0.7 ± 0.2 % at 1.4 Osm L^{-1}, **Table S3**). We also note that the magnitude of the difference between the fit and the observed data increased steadily as osmolarity decreased (**Figure S8**). This can be readily seen in **Figure 3A**, where the single exponential decay fit is in much better agreement with the data for 1.0 or 1.4 Osm L^{-1} than for 0.2 or 0.9 Osm L^{-1}. We speculate that these data suggest a secondary process occurs during electroporation of liposomes at greater initial membrane tension, e.g. a fluctuating fusion pore structure.

Redox Concentration in Liposomes Depends on Osmolarity of the Buffer. Looking at **Figure 3A**, it is obvious that peaks were larger in amplitude and longer in duration at 0.9 Osm L^{-1} than at 0.2 Osm L^{-1}, implying that more redox molecules are released from liposomes under this experimental condition. One can quantify the number of molecules ($N_{molecules}$) released per liposome collision/electroporation event using Faraday's equation: $N_{molecules} = Q/nF \times N_A$, where Q is the integrated charge from each amperometric event, n is the number of electrons transferred per molecule (1 e^- for $Fe(CN)_6^{4-}$), F is Faraday's constant (96485 C mol^{-1}), and N_A is Avogadro's number. When we analyzed the events at each osmolarity, we found surprising non-monotonic behavior, with $N_{molecules}$ per event reaching a maximum of 248,000 ± 17,400 molecules at 0.9 Osm L^{-1}; at the extremes, $N_{molecules}$ = 143,000 ± 8,100 at 0.2 Osm L^{-1} and $N_{molecules}$ = 101,000 ± 13,300 at 1.4 Osm L^{-1} ($p = 2.2 \times 10^{-16}$, ANOVA) (**Figure 4A**).

What is the mechanism for this behavior? A recent detailed study from the Rangamani group showed that when GUVs (radius 8, 14, or 20 μm) loaded with 200 mM sucrose were exposed to hypotonic buffer devoid of osmolytes, they initiated "swell-burst" cycles; hypotonic swelling due to H_2O influx increased GUV membrane tension to the point of rupture, permitting solution exchange.[28] Rupture events opened pores with radii as large as ~10 μm (GUV radius 20 μm), which resealed in about 100 ms. Cycles of swelling and bursting continued until the concentration differential between the inside and outside of the GUV was <10 mM.

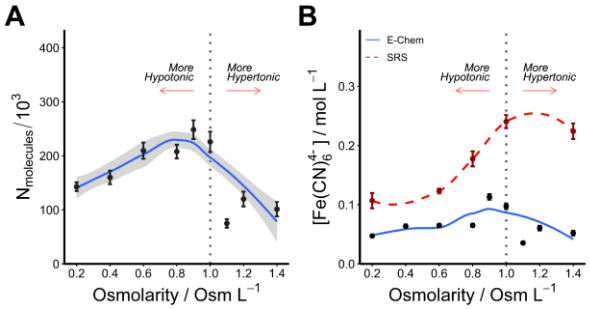

Figure 4. Osmolarity controls liposome redox concentration. *A)* Scatter plot of the $N_{molecules}$ detected per amperometric event from liposomes suspended in different osmolarity buffers. The blue curve (grey shading is SEM) is a local regression line which guides the eye to the non-monotonic behavior of $Fe(CN)_6^{4-}$ release. $p = 2.2 \times 10^{-16}$, ANOVA. *B)* Scatter plot of estimated $[Fe(CN)_6^{4-}]$ per liposome based on electrochemical detection (E-Chem) or stimulated Raman scattering (SRS). The blue curve (E-Chem) and dashed red curve are local regression lines (SEM omitted) to guide the eye. For E-Chem, $p = 2.2 \times 10^{-16}$, ANOVA. For SRS, $p = 5.8 \times 10^{-15}$, ANOVA.

If swell-burst cycles can also regulate osmolyte concentration in our 200 nm liposomes, then we reasoned that liposomes would release fewer molecules under more hypotonic conditions due to decreased internal $[Fe(CN)_6^{4-}]$. Indeed, from amperometric signals and DLS, we estimated that liposomes contained $[Fe(CN)_6^{4-}]$ = 47.5 ± 1.4 mM at 0.2 Osm L^{-1}, compared to 112 ± 4.2 mM at 0.9 Osm L^{-1}. However, estimated $[Fe(CN)_6^{4-}]$ also decreased under hypertonic conditions (54.4 ± 2.8 mM at 1.4 Osm L^{-1}),

when we expected the internal $[Fe(CN)_6^{4-}]$ to be stable (**Figure 4B**); this implies that liposome collision/electroporation events do not always result in complete electrolysis of liposome contents.

To more directly probe how liposome $[Fe(CN)_6^{4-}]$ changes in response to osmotic pressure, we used an orthogonal analytical technique, stimulated Raman scattering (SRS) microscopy. SRS microscopy is able to probe liposome contents label-free, by measuring the vibrational signature of $Fe(CN)_6^{4-}$ and correlating the signal intensity to a known $[Fe(CN)_6^{4-}]$ standard (see *Supporting Information*, **Figure S9**). As expected, SRS revealed that the internal $[Fe(CN)_6^{4-}]$ changed significantly with osmolarity, from $[Fe(CN)_6^{4-}]$ = 107 ± 12.8 mM at 0.2 Osm L^{-1} to 224 ± 13.2 mM at 1.4 Osm L^{-1} ($p = 5.8 \times 10^{-15}$, ANOVA).

Assuming the SRS determination of $[Fe(CN)_6^{4-}]$ in liposomes to be ground truth, amperometry detected 44.2 ± 1.5 % of the total contents at 0.2 Osm L^{-1}, which decreased to only 23.2 ± 1.8 % at 1.4 Osm L^{-1} (**Table S4**). Consequently, we believe liposomes can release a fraction of their total contents during electroporation, the magnitude of which depends on the initial membrane tension on the liposome.

Multipeak Detection of Single Liposomes. If liposomes can release a fraction of their total contents during amperometric detection, it stands to reason that liposomes may sometimes be detected multiple times, as was recently suggested by the Mirkin group.[27] Consistent with this hypothesis, we observed high frequency barrages of amperometric signals that far exceeded the expected rate, similar to what our group observed with Ag nanoparticle collision (**Figure 5**).[39] To capture this behavior quantitatively, we diluted liposomes 1000× in buffers ranging from 0.2-1.0 Osm L^{-1} (more hypertonic conditions gave rise to extremely low detection frequencies, data not shown) and recorded liposome collisions for 10 minutes. The Poisson probability that each amperometric event occurred due to an independent particle collision is given by:

$$P(t) = \frac{rt^k e^{-rt}}{k!}$$

where t is the arbitrary time interval (s), r is the overall frequency of events (s^{-1}), and k is the number of events occurring during the time interval.

Figure 5 shows selected traces featuring multipeak behavior with *P(t)* calculated manually. We observed as many as 13 events in 1.48 s (r = 0.213 s^{-1} for this trace) for a calculated $P(t) = 1.16 \times 10^{-11}$ that these were due to 13 independent particles. One can

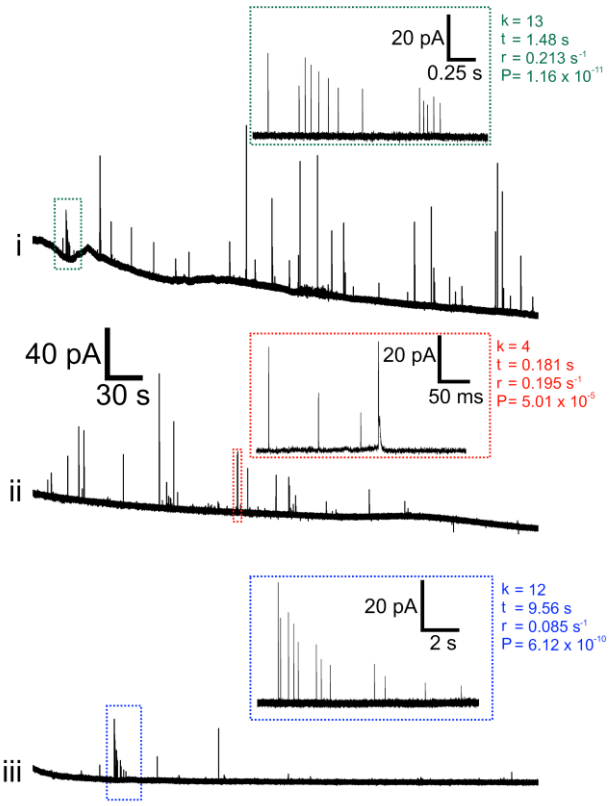

Figure 5. Multipeak behavior in Redox-Filled Liposomes. *A)* Amperometric traces showing multipeak behavior. Insets show selected high frequency bursts of events, with corresponding calculations of Poisson probability, *P*. *k* is the number of events, *t* is the time window in the inset, and *r* is the overall frequency of events for the entire trace. Experiment conditions for traces *i*: 0.6 Osm L^{-1}, *ii*: 0.8 Osm L^{-1}, *iii*: 1.0 Osm L^{-1}.

automate this analysis by setting t to the interspike interval[40] and k = 2; then, each event is associated with a Poisson probability, *P*. Interestingly, we found a population of events that occurred frequently though their calculated Poisson probability was low ($P < 1 \times 10^{-4}$). Their prevalence at all osmolarities tested was ~25% though the expected incidence was only 0.5% based on simulation (**Figure S10**, **Table S5**). We did not observe a statistically significant difference between probability distributions depending on osmolarity (p = 0.397, ANOVA). For a more detailed discussion of the statistical basis for classifying multipeak behavior, see **Supplementary Note 1**.

We believe that these low probability signals correspond to multiple detections of a single liposome. Liposomes do not appear to release their entire contents during electroporation (**Figure 4**). These low probability signals do not depend on osmolarity, implying that multipeak behavior arises

through a separate mechanism. It is possible that multipeak behavior may be related to multilamellarity, which has been observed in liposomes synthesized under similar conditions.[41] It is also possible that multipeak events arise due to collision of aggregates of multiple liposomes. We plan to study this phenomenon in greater detail in a future work.

CONCLUSION

In conclusion, we used amperometry and CFE to study single, 200 nm liposomes loaded with redox molecules. We found the liposome detection frequency depended strongly on the liposome membrane tension, consistent with detection *via* electroporation. The size of the fusion pore that formed during liposome electroporation also depended on membrane tension, with tense membrane conditions favoring wider fusion pores.

Critically, the concentration of redox molecules inside liposomes was regulated by the osmolarity of the external solution, confirmed by both amperometry and SRS. We suspect that this dynamic control of liposome contents is related to "swell-burst cycles," a phenomenon observed in GUVs. The disparity between the concentration estimates from amperometry and SRS support that liposomes only release a fraction of their contents during electroporation, i.e. they may open and close more than once. We provide statistical evidence for such "multipeak" behavior. This study improves the understanding of how liposomes accumulate molecules and release them during electroporation, which may be relevant to vesicle analysis or the development of rapid, quantitative techniques for characterizing liposomes.

SUPPORTING INFORMATION

Experimental details on dynamic light scattering (DLS), stimulated Raman scattering (SRS) microscopy, statistics on peak characteristics, calculated pore characteristics, loading, and multipeak behavior, as well as a detailed discussion of estimating Poisson probabilities and additional details about the SRS experiment may all be found in the Supporting Information.

AUTHOR INFORMATION

Corresponding Author

Bo Zhang

Department of Chemistry, University of Washington, Seattle WA 98195-1700 United States

email: zhangb@uw.edu

Author Contributions

S.T.B., B.F., D.F., and B.Z. designed experiments. S.T.B., B.F. performed experiments. S.T.B., B.F. analyzed the data. S.T.B., B.F., and B.Z. wrote the manuscript. All authors have given approval to the final version of the manuscript.

Funding Sources

This work was supported by the National Science Foundation (CHE-1904426) to S.B. and B.Z. This work was funded in parts by the NSF CAREER 1846503 to D.F. and NSF GRF DGE-12560682 to B.F.

ACKNOWLEDGMENT

The authors would first like to thank Caitlin E. Cornell and the Sarah L. Keller lab at the University of Washington (UW) for their assistance in understanding membrane biophysics. The authors thank the Joshua Vaughan lab at UW for generously providing access to their centrifuge for the isolation of redox-filled liposomes. The authors also thank the Daniel Chiu lab at UW for their assistance with dynamic light scattering.

REFERENCES

1. Sezgin, E.; Kaiser, H. J.; Baumgart, T.; Schwille, P.; Simons, K.; Levental, I. "Elucidating membrane structure and protein behavior using giant plasma membrane vesicles." *Nat. Protocols*, **2012**, *7*, 1042–1051.
2. Baumgart, T.; Hammond, A. T.; Sengupta, P.; Hess, S. T.; Holowka, D. A.; Baird, B. A.; Webb, W. W. "Large-scale fluid/fluid phase separation of proteins and lipids in giant plasma membrane vesicles." *Proc. Nat. Acad. Sci.*, **2007**, *104*, 3165–3170.
3. Cornell, C. E.; McCarthy, N. L. C.; Levental, K. R.; Levental, I.; Brooks, N. J.; Keller, S. L. "n-Alcohol Length Governs Shift in Lo-Ld Mixing Temperatures in Synthetic and Cell-Derived Membranes." *Biophys. J.* **2017**, *113*, 1200–1211.
4. Cornell, C. E.; Skinkle, A. D.; He, S.; Levental, I.; Levental, K. R.; Keller, S. L. "Tuning Length Scales of Small Domains in Cell-Derived Membranes and Synthetic Model Membranes." *Biophys. J.*, **2018**, *115*, 690–701.
5. Kahya, N.; Scherfeld, D.; Bacia, K.; Schwille, P. "Lipid domain formation and dynamics in giant unilamellar vesicles explored by fluorescence correlation spectroscopy." *J. Struct. Biol.,* **2004**, *147*, 77–89.
6. Lingwood, D. & Simons, K. "Lipid rafts as a membrane-organizing principle." *Science*, **2010**, *327*, 46–50.
7. Dimova, R.; Riske, K. A.; Aranda, S.; Bezlyepkina, N.; Knorr, R. L.; Lipowsky, R. "Giant vesicles in electric fields." *Soft Matter*, **2007**, *3*, 817–827.
8. Dimova, R.; Bezlyepkina, N.; Jordö, M. D.; Knorr, R. L., Riske, K. A.; Staykova, M.; Vlahovska, P. M.; Yamamoto, T.; Yang, P.; Lipowsky, R. "Vesicles in electric fields: Some novel aspects of membrane behavior." *Soft Matter*, **2009**, *5*, 3201–3212.
9. Riske, K. A. & Dimova, R. (2005). "Electro-deformation and poration of giant vesicles viewed with high temporal resolution." *Biophys. J.*, **2005**, *88*, 1143–1155.
10. Jahn, R.; Lang, T.; Südhof, T. C. "Membrane fusion." *Cell*, **2003**, *112*, 519–533.
11. Kliesch, T. T.; Dietz, J.; Turco, L.; Halder, P.; Polo, E.; Tarantola, M.; Jahn, R.; Janshoff, A. "Membrane tension increases fusion efficiency of model membranes in the presence of SNAREs." *Sci. Rep.*, **2017**, *7*, 1–13.
12. Witkowska, A., & Jahn, R. "Rapid SNARE-Mediated Fusion of Liposomes and Chromaffin Granules with Giant Unilamellar Vesicles." *Biophys. J.*, **2017**, *113*, 1251–1259.
13. Mühlenbrock, P.; Herwig, K.; Vuong, L.; Mey, I.; Steinem, C. "Fusion Pore Formation Observed during SNARE-Mediated Vesicle Fusion with Pore-Spanning Membranes." *Biophys. J.*, **2020**, *119*, 151–161.
14. Mosharov, E. V. & Sulzer, D. "Analysis of single-vesicle exocytotic events recorded by amperometry." *Nat. Methods*, **2008**, *2*, 651–658.
15. Hellberg, D.; Scholz, F.; Schauer, F.; Weitschies, W. "Bursting and spreading of liposomes on the surface of a static mercury drop electrode." *Electrochem. Comm.* **2002**, *4*, 305–309.
16. Hellberg, D.; Scholz, F.; Schubert, F.; Lovrić, M.; Omanović, D.; Hernández, V. A.; Thede, R. "Kinetics of liposome adhesion on a mercury electrode." *J. Phys. Chem. B*, **2005**, *109*, 14715–14726.
17. Liu, Y.; Xu, C.; Yu, P.; Chen, X.; Wang, J.; Mao, L. "Counting and Sizing of Single Vesicles/Liposomes by Electrochemical Events." *ChemElectroChem*, **2018**, *5*, 2954–2962.
18. Plant, A. L.; Gueguetchkeri, M.; Yap, W. "Supported phospholipid/alkanethiol biomimetic membranes: insulating properties." *Biophys. J.*, **1994**, *67*, 1126–1133.
19. Wilburn, J. P.; Wright, D. W.; Cliffel, D. E. "Imaging of voltage-gated alamethicin pores in a reconstituted bilayer lipid membrane via scanning electrochemical microscopy." *Analyst*, **2006**, *131*, 311–316.
20. Campos, R. & Kataky, R. "Electron transport in supported and tethered lipid bilayers modified with bioelectroactive molecules." *J. Phys. Chem. B*, **2012**, *116*, 3909–3917.
21. Schmallegger, M.; Barbon, A.; Bortolus, M.; Chemelli, A.; Bilkis, I.; Gescheidt, G.; Weiner, L. "Systematic Quantification of Electron Transfer in a Bare Phospholipid Membrane Using Nitroxide-Labeled Stearic Acids: Distance Dependence, Kinetics, and Activation Parameters." *Langmuir*, **2020**, *36*, 10429–10437.
22. Lebègue, E.; Anderson, C. M.; Dick, J. E.; Webb, L. J.; Bard, A. J. "Electrochemical Detection of Single Phospholipid Vesicle Collisions at a Pt Ultramicroelectrode." *Langmuir*, **2015**, *31*, 11734–11739.
23. Lebègue, E.; Barrière, F.; Bard, A. J. "Lipid Membrane Permeability of Synthetic Redox DMPC Liposomes Investigated by Single Electrochemical Collisions." *Anal. Chem.*, **2020**, *92*, 2401–2408.
24. Cheng, W. & Compton, R. G. "Investigation of single-drug-encapsulating liposomes using the nano-impact method." *Angew. Chem. Int. Ed.*, **2014**, *53*, 13928–13930.
25. Lovrić, J.; Najafinobar, N.; Dunevall, J.; Majdi, S.; Svir, I.; Oleinick, A.; Amatore, C.; Ewing, A. G. "On the mechanism of electrochemical vesicle cytometry: chromaffin cell vesicles and liposomes." *Faraday Discussions*, **2016**, *193*, 65–79.
26. Barlow, S. T. & Zhang, B. "Fast Detection of Single Liposomes Using a Combined Nanopore Microelectrode Sensor." *Anal. Chem.*, **2020**, *92*, 11318–11324.
27. Pan, R.; Hu, K.; Jiang, D.; Samuni, U.; Mirkin, M. V. "Electrochemical Resistive-Pulse Sensing." *J. Am. Chem. Soc.*, **2020**, *141*, 19555–19559.
28. Chabanon, M., Ho, J. C. S., Liedberg, B., Parikh, A. N., & Rangamani, P. "Pulsatile Lipid Vesicles under Osmotic Stress." *Biophys. J.*, **2017**, *112*, 1682–1691.
29. Li, X.; Majdi, S.; Dunevall, J.; Fathali, H.; Ewing, A. G. "Quantitative Measurements of Transmitters in Vesicles One at a Time in Single Cell Cytoplasm with Nano-tip Electrodes." *Angew. Chem. Int. Ed.*, **2015**, *54*, 11978–11982.
30. Dunevall, J.; Fathali, H.; Najafinobar, N.; Lovric, J.; Wigström, J.; Cans, A. S.; Ewing, A. G. "Characterizing the Catecholamine Content of Single Mammalian Vesicles by Collision-Adsorption Events at an Electrode." *J. Am. Chem. Soc.*, **2015**, *137*, 4344–4346.
31. Dunevall, J.; Majdi, S.; Larsson, A.; Ewing, A. G. "Vesicle impact electrochemical cytometry compared to amperometric exocytosis measurements." *Curr. Opin. Electrochem.*, **2017**, *5*, 85–91.
32. Li, X.; Ren, L.; Dunevall, J.; Ye, D.; White, H. S.; Edwards, M. A.; Ewing, A. G. "Nanopore Opening at Flat and Nanotip Conical Electrodes during Vesicle Impact Electrochemical Cytometry." *ACS Nano*, **2018**, *12*, 3010–3019.
33. Zhang, X. W.; Hatamie, A.; Ewing, A. G. "Simultaneous Quantification of Vesicle Size and Catecholamine Content by Resistive Pulses in Nanopores and Vesicle Impact Electrochemical Cytometry." *J. Am. Chem. Soc.*, **2020**, *142*, 4093–4097.
34. Barlow, S. T.; Louie, M.; Hao, R.; Defnet, P. A.; Zhang, B. "Electrodeposited Gold on Carbon-Fiber Microelectrodes for Enhancing Amperometric Detection of Dopamine Release from Pheochromocytoma Cells." *Anal. Chem.*, **2018**, *90*, 10049–10055.
35. Bard, A. J.; Faulkner, L. R. *Electrochemical Methods: Fundamentals and Applications*; John Wiley & Sons, 2000.

36. Hoffmann, E. K.; Lambert, I. H.; Pedersen, S. F. Physiology of cell volume regulation in vertebrates. *Physiol. Rev.*, **2009**, *89*, 193–277.

37. Oleinick, A.; Lemaître, F.; Collignon, M. G.; Svir, I.; Amatore, C. "Vesicular release of neurotransmitters: Converting amperometric measurements into size, dynamics and energetics of initial fusion pores." *Faraday Discussions*, **2013**, *164*, 33–55.

38. Konopka, S. J.; McDuffie, B. "Diffusion Coefficients of Ferri- and Ferrocyanide Ions in Aqueous Media, Using Twin-Electrode Thin-Layer Electrochemistry." *Anal. Chem.*, **1970**, *42*, 1741–1746.

39. Oja, S. M.; Robinson, D. A.; Vitti, N. J.; Edwards, M. A.; Liu, Y.; White, H. S.; Zhang, B. "Observation of multipeak collision behavior during the electro-oxidation of single ag nanoparticles." *J. Am. Chem. Soc.*, **2017**, *139*, 708–718.

40. Bruns, D.; Riedel, D.; Klingauf, J.; Jahn, R. "Quantal release of serotonin." *Neuron*, **2000**, *28*, 205–220.

41. Scott, H. L.; Skinkle, A.; Kelley, E. G.; Waxham, M. N.; Levental, I.; Heberle, F. A. "On the Mechanism of Bilayer Separation by Extrusion, or Why Your LUVs Are Not Really Unilamellar." *Biophys. J.*, **2019**, *117*, 1381–1386.

For TOC only